Probing a Water Channel near the A-Ring of Receptor-Bound 1α,25-Dihydroxyvitamin D3 with Selected 2α-Substituted Analogues †

7 AUTHORS, INCLUDING:

Atsushi Kittaka
Teikyo University
164 PUBLICATIONS **1,942** CITATIONS

Yoshitomo Suhara
Shibaura Institute of Technology
81 PUBLICATIONS **2,217** CITATIONS

Natacha Rochel
Institut de Génétique et de Biologie Molécula…
81 PUBLICATIONS **3,859** CITATIONS

Dino Moras
Institut de Génétique et de Biologie Molécula…
459 PUBLICATIONS **27,769** CITATIONS

Probing a Water Channel near the A-Ring of Receptor-Bound 1α,25-Dihydroxyvitamin D3 with Selected 2α-Substituted Analogues[†]

Shinji Hourai,[‡,§] Toshie Fujishima,[#] Atsushi Kittaka,[#] Yoshitomo Suhara,[#] Hiroaki Takayama,[#] Natacha Rochel,[‡] and Dino Moras*,[‡]

Laboratoire de Biologie et Génomique Structurales, UMR 7104, Institut de Génétique et de Biologie Moléculaire et Cellulaire, CNRS/INSERM/ ULP, 1, Rue Laurent Fries, BP 10142, 67404 Illkirch Cedex, France, and Department of Pharmaceutical Chemistry, Faculty of Pharmaceutical Sciences, Teikyo University, Sagamiko, Kanagawa 199-0195, Japan

The crystal structure of the vitamin D receptor (VDR) in complex with 1α,25(OH)$_2$D$_3$ revealed the presence of several water molecules near the A-ring linking the ligand C-2 position to the protein surface. Here, we report the crystal structures of the human VDR ligand binding domain bound to selected C-2α substituted analogues, namely, methyl, propyl, propoxy, hydroxypropyl, and hydroxypropoxy. These specific replacements do not modify the structure of the protein or the ligand, but with the exception of the methyl substituent, all analogues affect the presence and/or the location of the above water molecules. The integrity of the channel interactions and specific C-2α analogue directed additional interactions correlate with the binding affinity of the ligands. In contrast, the resulting loss or gain of H-bonds does not reflect the magnitude of HL60 cell differentiation. Our overall findings highlight a rational approach to the design of more potent ligands by building in features revealed in the crystal structures.

Introduction

The vitamin D nuclear receptor belongs to the superfamily of steroid/thyroid hormone/retinoid nuclear receptors and acts as a ligand-dependent transcriptional modulator to control multiple cellular responses including, growth, apoptosis, angiogenesis, antiproliferation, and differentiation.[1−4] VDR[a] mediates the genomic actions upon binding to 1α,25-dihydroxyvitamin D3, the active form of the seco-steroid hormone vitamin D.[5] In addition, 1α,25-dihydroxyvitamin D3 exerts an important role in the regulation of bone development/metabolism and calcium homeostasis.[6−7]

Therapeutic applications of 1α,25(OH)$_2$D$_3$ analogues are treatments for renal osteodystrophy, osteoporosis, psoriasis, cancer, autoimmune diseases, and prevention of graft rejection. The calcemic effects induced by 1α,25(OH)$_2$D$_3$ causing hypercalcemia, increased bone resorption, and soft tissue calcification limit the use of the natural ligand in these clinical applications. Therefore, analogues with reduced side effects are developped.[3] Chemical modifications are operated on the A and/or CD rings or aliphatic side chain and lead to analogues that exhibit specific properties.[8]

The previously reported crystal structures of human VDR in complex with 1α,25(OH)$_2$D$_3$ (**A**) and several synthetic ligands[9−11] revealed the presence of tightly bound water molecules forming a channel near the C-2 position of the ligand (Figure 1). This additional space could be used to accommodate modified analogues in the ligand binding pocket (LBP). To date, a variety of A-ring modified analogues were synthesized and biologically characterized.[12−17] Attempts to correlate the binding affinity with the bulkiness of the ligands have been unsuccessful. To elucidate the role of water molecules and the resulting structure−activity relationship, we determined crystal structures of VDR in complex with five selected 2α-substituted 1α,25-dihydroxyvitamin D$_3$ analogues. These α,25-dihydroxyvitamin D$_3$ analogues have substituent groups at C-2 (methyl (**B**), propyl (**C**), propoxy (**D**), hydroxypropoxyl (**E**), hydroxypropoxy (**F**) (Figure 2). These new crystal structures allow a correlation between the A-ring substitutions with VDR affinity and provide a structural basis for the functional importance of the water channel molecules.

Results and Discussion

Crystal Structures. Crystals of the five complexes were grown using the human VDR LBD mutant lacking 50 residues in the loop that connects helices H1 and H3. The same construct was previously used to solve the structure of the VDR LBD bound to 1α,25(OH)$_2$D$_3$ and several synthetic ligands.[9−11] This mutant exhibits the same biological properties (binding, transactivation in several cell lines, heterodimerization) as the VDR LBD wild type.[18] An additional advantage of this mutant is that its crystal packing and thus crystallization conditions are very sensitive to any conformational change that affects the ligand binding pocket and the coactivator binding site. Crystal growth is then a clear indication of lack of large conformational changes. For each complex the crystals were obtained under conditions similar to those used for the complex with the natural ligand and were isomorphous. The crystallographic data are summarized in Supporting Information. The omit maps from the refined atomic model of VDR LBD were used to fit the ligands to their electron density. Each map shows an unambiguous electron density to fit the ligand (Figure 3a).

The VDR complexes with C-2α substituents (**B−F**) adopt the canonical conformation of all previously reported agonist-
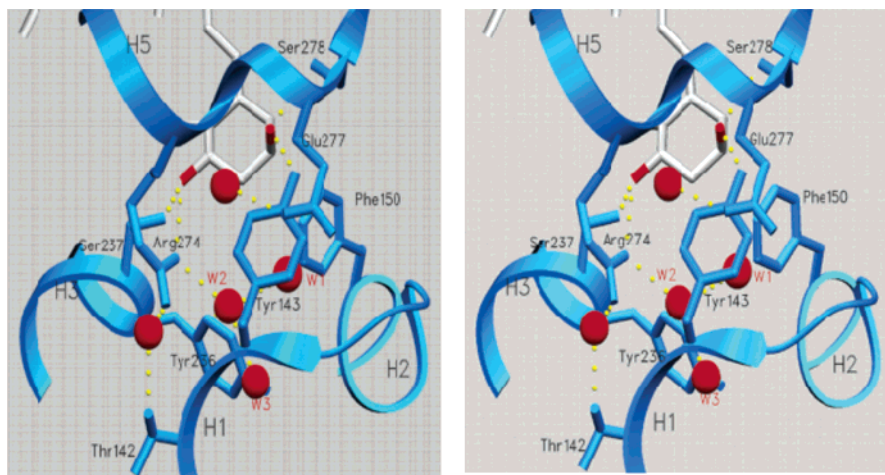

Figure 1. Stereoview of the water channel in the LBP of VDR. The view is restricted to the region of the water molecules surrounding the A-ring of $1\alpha,25(OH)_2D_3$. The water molecules are shown as red spheres. Residue side chains closer than 4.0 Å are shown. The $1\alpha,25(OH)_2D_3$ is shown in stick representation with carbon and oxygen atom in gray and red, respectively. The hydrogen bonds formed by the ligands and those formed by the water molecules are shown as yellow dotted lines.
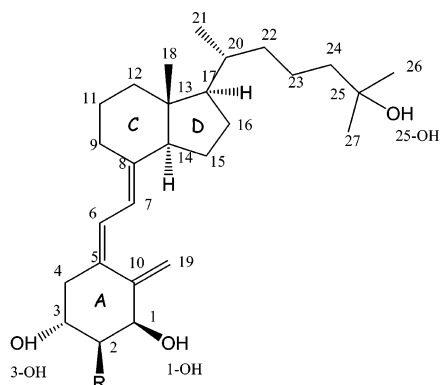
Ligand	Chemical Structure of R
$1\alpha,25(OH)_2D_3$ (R = H) (**A**)	H
Methyl (R = CH3) (**B**)	C-28
1-Propyl (R = $CH_2CH_2CH_3$) (**C**)	C-28, C-30, C-29
1-Propoxy (R =, $OCH_2CH_2CH_3$) (**D**)	C-2 O, C-29, C-28, C-30
3-Hydroxy-1-propyl (R =, $CH_2CH_2CH_2OH$) (**E**)	C-28, C-30, C-29, OH, 30-OH
3-Hydroxy-1-propoxy (R = $OCH_2CH_2CH_2OH$) (**F**)	C-2 O, C-29, OH, 30-OH, C-28, C-30

Figure 2. Chemical structures of 2α-substituted $1\alpha,25$-dihydroxyvitamin D_3 analogues. **A** is $1\alpha,25(OH)_2D_3$ ($1\alpha,25$-dihydroxyvitamin D_3). **B** is 2α-methyl-$1\alpha,25$-dihydroxyvitamin D_3. **C** is 2α-propyl-$1\alpha,25$-dihydroxyvitamin D_3. **D** is 2α-propoxy-$1\alpha,25$-dihydroxyvitamin D_3. **E** is 2α-(3-hydroxypropyl)-$1\alpha,25$-dihydroxyvitamin D_3. **F** is 2α-(3-hydroxypropoxy)-$1\alpha,25$-dihydroxyvitamin D_3.

bound nuclear receptor LBD.[19] The position and conformation of the activation helix 12 are strictly maintained. The high level of structural homology is reflected by the very low value of the root-mean-squared deviation (rmsd). When compared to VDR−$1\alpha,25(OH)_2D_3$ complex, the rmsd on Cα atoms is 0.19, 0.33, 0.29, 0.23, and 0.32 Å for VDR complexes with **B**, **C**, **D**, **E**, and **F**, respectively.

The side chain conformations of some residues differ from those described for the VDR LBD−$1\alpha,25(OH)_2D_3$ structure, but variations concern mainly side chains located at the surface of the protein and the region of loop 9−10. Phe-150, which forms a weak van der Waals contact with the 2α-substituent of ligands, is the only residue close to the C-2α position that exhibits small differences between the various structures. The A-, seco-B, C-, and D-rings and the 17β-aliphatic side chain form similar contacts in VDR−$1\alpha,25(OH)_2D_3$ complexes with methyl, propyl, propoxy, hydroxypropyl, and hydroxypropoxy substituents. The volume of the ligands varies from 382 to 421 Å^3, compared with 366 Å^3 for $1\alpha,25(OH)_2D_3$ and 392 Å^3 for KH1060, a superagonist whose structure is closely related to that of secocalcitol.[11] Removal of water molecules is the solution that allows accommodation of the volume changes at the specific location near C-2α without changing significantly the overall structure of the LBD.

^{1}H NMR analysis and molecular mechanics calculation showed that the A-ring of 2α-methyl-$1\alpha,25(OH)_2D_3$ is in equilibrium between chair α and β conformations. The α form is predominant over that of the β one.[20,21] In the crystal structures, the A-ring adopts β chair conformation with the 19-methylene group "up" and the 1-OH and 3-OH groups in an equatorial and axial orientation, respectively. The hydrogen bonds for 1-OH and 3-OH consist of Ser-237/Arg-274 and Tyr-143/Ser-278, respectively. These results are consistent with those observed with human VDR bound to $1\alpha,25(OH)_2D_3$[9] and synthetic agonists or superagonists[10,11] as well as rat VDR in complex with 2α-methyl or methylene substituted analogues.[22] Interestingly, the 2-methylene,19-nor vitamin D ligand bound to rat VDR[22] superposes to the 2α-methyl analogue, despite the absence of the methylene group. This observation stresses the importance of the H-bonds for the position and the stability of the ligand and suggests that the loss of van der Waals contacts between the C-19 methylene group and two residues explains the lower stability.

The conformations of the bound ligands are shown in Figure 3a, and the superposition of the A-ring with the associated water moleculesis is reported in Figure 3b. The propyl and hydroxypropyl substituents adopt a near-staggered conformation (torsion angles of C-1−C-2−C-28−C-29 are −179° and −171.3° for **C** and **E**, respectively). In contrast, the propoxy and hydroxypropoxy substituents adopt a near-anticlinal conforma-
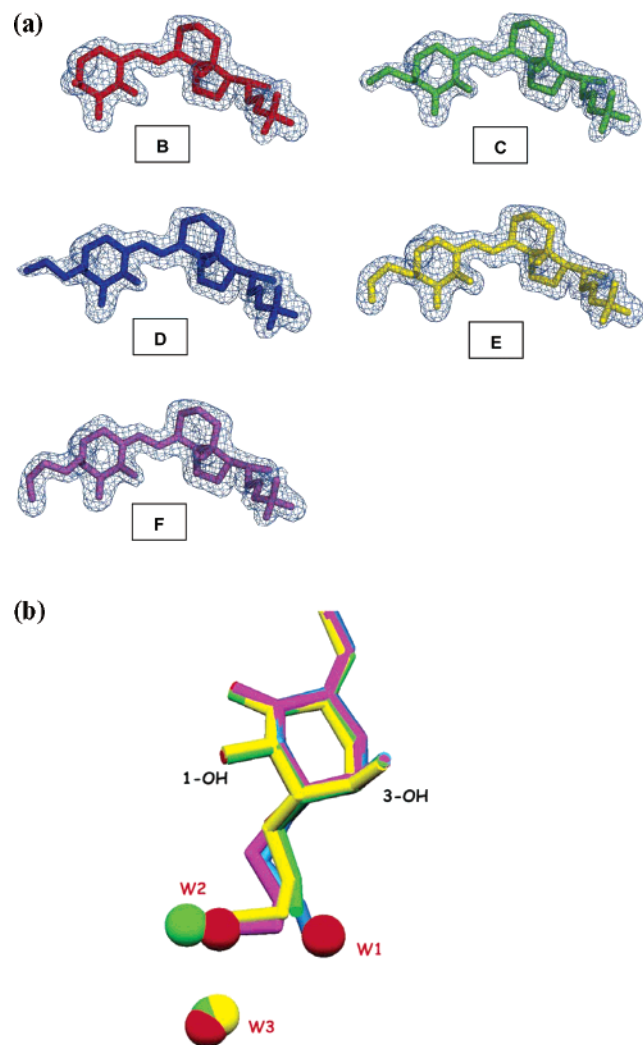
Figure 3. Conformation of the bound ligands. (a) The δ_A-weighted $F_o - F_c$ omit map is shown contoured at 2.5 δ (blue). The ligands **B** (red), **C** (green), **D** (blue), **E** (yellow), and **F** (magenta) are shown in stick representation. (b) Close-up view of the substituted chain group of ligands **B** (red), **C** (green), **D** (blue), **E** (yellow), and **F** (magenta) after superimposed VDR complexes. Water molecules (W1, W2, W3) are shown as spheres in the same color as each ligand.

Figure 4. Close-up view of the water molecules network near C-2 position of ligands. Shown are VDR complexes with **A** (a), **B** (b), **C** (c), **D** (d), **E** (e), and **F** (f) substituents. The water molecules are shown as red spheres. The missing water molecules in **C**−**F** complexes are shown as dotted lines to red spheres. Residue side chains contacting the water molecules through H-bonds are shown. The ligands are shown in stick representation with carbon and oxygen atom in gray and red, respectively. The hydrogen bonds formed by the ligands and those formed by the water molecules are shown as yellow dotted lines.

tion (torsion angles of C-1−C-2−O−C-28 are −110° and −96.5° for **D** and **F**, respectively).

The Water Molecules Network. We compared the water network around the A-ring of receptor-bound 1α,25-dihydroxyvitamin D3 with that obtained with selected 2α-substituted analogues (Figure 4). In the VDR-1α,25(OH)$_2$D$_3$ complex structure,[9] three water molecules (W1, W2, and W3) form a channel leading to the C-2 position of ligand (Figures 1 and 4a). They are present in all crystal structures of hVDR complexes. Notably the presence and the position of the water molecules are strictly conserved in zVDR[23] and rVDR[22] complexes. The channel connects the A-ring part of the LBP to the surface of the protein and forms a network of H-bonds (Figure 1). Within these water molecules, W1, W2, and W3 are affected by the 2α-substituted analogues. The *B*-factors, which reflect the mobility of these three buried water molecules (30.6, 21.5, and 20.3 Å^2 for W1, W2, and W3, respectively, for the VDR−1α,25(OH)$_2$D$_3$ complex) are significantly lower than the average value of all water molecules (45.5 Å^2), suggesting that these water-bound molecules play an important role in protein folding and stability. W1 makes hydrogen bonds with W2 and the carbonyl group of Asp-144. In addition, W2
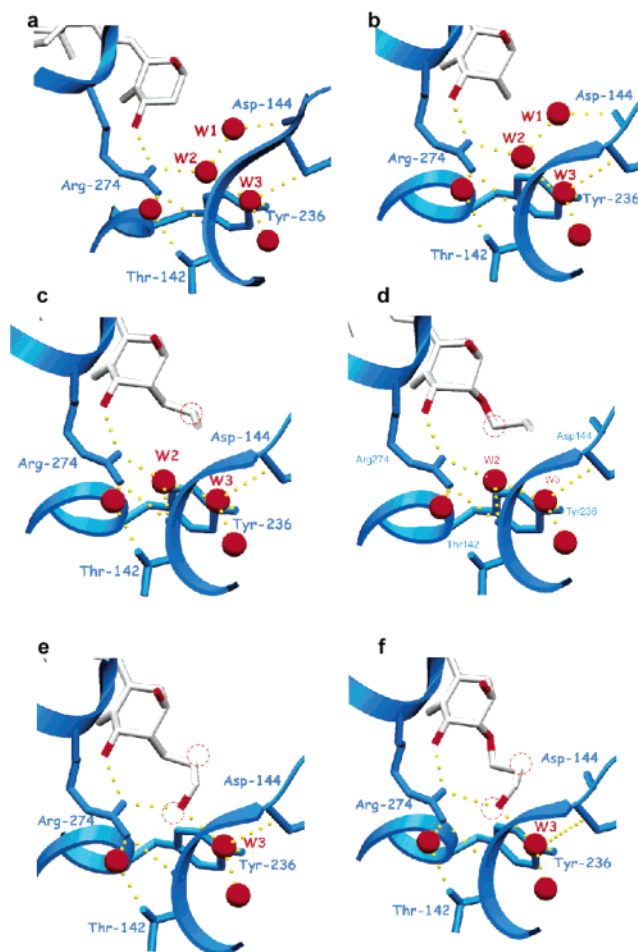
makes hydrogen bond with Arg-274, an important residue for the stabilization of VDR LBD ligand complexes and W3, which itself interacts with the hydroxyl group of Tyr-236. Other water molecules close to the site are always visible in the electron density map and are not affected by the analogues. One interacts with Arg-274 and Thr-142 at the end of H1 (Figure 1). The Arg-274 water channel region, like the solvent-exposed His-rich region, may be stabilized[24] by the mildly acidic pH of the crystallization conditions of hVDR LBD. Note that the H-bond networks involving the water molecules are important for the stability of loops near the A-ring.

The crystal structures of the human VDR LBD bound to the C-2α substituted analogues indicate that the presence or absence of W1, W2, and W3 depends on the nature of the 2α-substituted analogues. In the VDR−**B** complex structure, the substituted methyl group does not affect the position and interactions of these water molecules (Figure 4b). The lower *B*-factors of W1 (16.0 Å^2), W2 (12.5 Å^2), and W3 (11.6 Å^2) compared to the average for all water molecules (28.1 Å^2) reflect the stability of these three water molecules in the VDR LBP. In the VDR complexes with **C** and **D** (parts c and d of Figure 4), W1 molecules are replaced and W2 molecules are shifted by 1 Å (**C**) and 0.7 Å (**D**). Beside making hydrogen bonds with W3

and Arg-274, W2 establishes close contacts with the terminal methyl group of ligands (at 3.1 and 3.2 Å, respectively) (parts c and d of Figure 4). The higher *B*-factors of W2 (36.1 and 28.8 Å^2 for VDR−**C** and VDR−**D**) compared to those of W3 (18.3 and 17.0 Å^2 for VDR−**C** and VDR−**D**) indicate that W2 is slightly destabilized (see Supporting Information). In contrast, in the VDR complexes with **E** and **F**, both W1 and W2 are expelled with the terminal hydroxyl group of the ligands replacing W2 to form hydrogen bonds with VDR (parts e and f of Figure 4).

Ligand−Protein Interactions. The same van der Waals interactions as those described in the initial structure of VDR−1α,25(OH)$_2$D$_3$[9] are observed for the A, seco-B, C, and D rings and 17β-aliphatic side chain of the ligands **B**−**F**. The interaction made with Val-418 of H12 is conserved in all studied complexes. The hydroxyl groups 1-OH, 3-OH, and 25-OH make the same hydrogen bonds, 1-OH with Ser-237 and Arg-274, 3-OH with Tyr-143 and Ser-278, and 25-OH with His-305 and His-397. The specific interactions concern the C-2α groups of the ligands. All interactions and conclusions made on these structures of the hVDR mutant are relevant to the wild-type VDR. The ligand binding pocket and interactions made by the natural ligand are strictly identical in the structures of hVDRΔ and zVDR wild-type in complex with a coactivator peptide.[23]

In the VDR−**B** complex structure, the 2α-methyl group fills a small empty cavity in the LBD and makes additional weak van der Waals contacts with Phe-150, Leu-233, and Ser-237. These additional bonds of the **B** ligand compared to 1α,25-(OH)$_2$D$_3$ can explain the 4-fold increased affinity of **B** for VDR. In silico docking of a 2β-methyl group in VDR LBD indicates that for this conformer the methyl group makes bad contacts with Tyr-143. The resulting destabilization is likely to explain the marked decrease of the affinity of the 2β-methyl 1α,25-(OH)$_2$D$_3$.[25] In line with these observations, the 2-methylene group in the rVDR[22] crystal structure displays contacts similar to those of the 2α-methyl group in the hVDR LBD.

In the VDR−**C** complex structure, the side chain of Phe-150 is shifted by 1.0 Å and makes a weak van der Waals contact (3.8 Å) with C-29 of **C** ligand. Compared to 1α,25(OH)$_2$D$_3$ and **B** complexes, the **C** ligand makes additional contacts with the LBP. Those are weak van der Waals bonds between the propyl group at C-2 and Tyr-143, Asp-144, and Tyr-147. In the VDR−**D** complex structure, the propoxy group at C-2 contacts the same residues as **C** plus Tyr-236. However, for both **C** and **D** ligands the replacement of W1 by the hydrophobic CH$_2$ group results in the suppression of two H-bonds with Asp144 and W2, a loss of energy. Moreover, both **C** and **D** ligands induce a 1 Å shift of W2. Altogether, the balance of contacts and the destabilization of W2 can explain the lower binding affinity of **C** and **D** for VDR (Figure 5).

The hydroxypropyl and hydroxypropoxy groups of **E** and **F** contact Thr-142, Tyr-143, Asp-144, Tyr-147, Phe-150, Tyr-236, Ser-237, and Arg-274, and for **F** an additional contact is made with Leu-233. They replace both W1 and W2, but the terminal hydroxyl group occupies the place of W2 and restores the H-bonds with W3 and Arg-274. The overall balance of interactions is in favor of the analogues and can explain the higher binding affinities of ligands **E** and **F** for VDR (Figure 5). The observation that altering the water molecules near the guanidinium of Arg-274 affects affinity and functional potency suggests another interesting correlation. The Arg-274 mutation to Leu is known to cause vitamin D resistant rickets[29] and decreases the binding affinity of 1α,25(OH)$_2$D$_3$ by 3 orders of magnitude compared to wild-type VDR. The additional hydro-
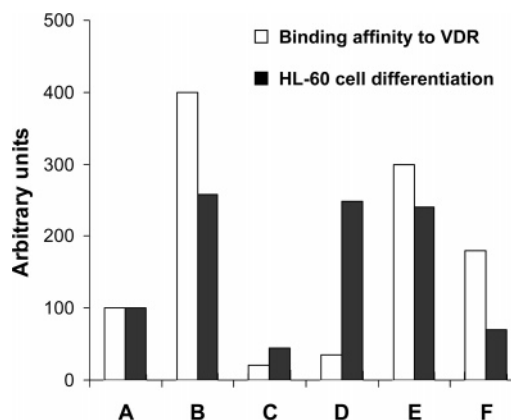

Figure 5. Binding affinity level of the five selected 2α-substituted analogues of 1α,25(OH)$_2$D$_3$ does not correlate with its capacity to induce HL-60 cell differentiation (previously published data[12,14,15] and new data). The potency of 1α,25(OH)$_2$D$_3$ was normalized to 100. Data are the mean of three separate experiments. Relative activity was calculated at EC$_{50}$. EC$_{50}$ is the concentration at half of NBT positive % at 10^{-6} M 1α,25(OH)$_2$D$_3$. Binding affinity to VDR of the ligands and their potential effects on HL-60 differentiation are represented by white and black bars, respectively.

gen bond formed by the terminal hydroxyl groups of the **F** ligand might compensate for the loss of hydrogen bond between 1α-OH and Arg-274 in Arg274Ala mutant VDR and consequently explains why that ligand shows higher binding affinity for Arg274Ala mutant VDR than 1α,25(OH)$_2$D$_3$.[30]

HL60 Cell Differentiation. To understand the functional role of the C-2α substituted analogues compared to the natural ligand, we checked whether the magnitude of their binding affinity correlates with their ability to induce HL60 differentiation into monocyte-like cells. Results presented in Figure 5 reveal distinct profiles between the binding affinity of hVDR−C-2α substituted analogues and HL60 cell differentiation. Although we observe a correlation between affinity and HL60 cell differentiation for **B**, **C**, and **E** compounds with an increased activity for ligands that bind better, it is the reverse for **D** and **F** ligands (Figure 5). The HL60 differentiation is markedly increased for **D** and slightly decreased for **F**, while their binding affinities are decreased for **D** and increased for **F** ligands. Using the same cellular model, Verlinden et al. observed a similar discrepancy with the 19-nor-*trans*-decalin-1α,25(OH)$_2$D$_3$ analogue.[26]

It is known that the binding affinity to VDR does not always correlate with transactivation efficiency.[27] The present results are in agreement with our observations for the superagonist ligands.[10] The lifetime of the active conformation is the main factor responsible for the formation of more potent complexes with coactivator and transcriptional activity. This hypothesis was further supported by the findings that the ability to induce stronger VDR−DRIP205/SRC1/TIF2 coactivator interactions is the basis for the superagonistic profiles of TX522 and TX527, two 14-epi analogues of 1α,25-dihydroxyvitamin D$_3$.[28] In summary, the strength of binding affinity to VDR and transactivation are two not necessarily related parameters that may participate in HL60 differentiation.

Conclusion

The crystal structures of VDR with 2α-substituted analogues provide a molecular explanation for the interaction between substituted chain groups (methyl, propyl, propoxy, hydroxypropyl, and hydroxypropoxy) and water molecules. Such an analysis underscores the importance of the water channel network for

increased stability. The C-2α groups modulate the affinity for VDR by changes in protein or water contacts.

In each complex the protein structure and the conformation of ligands from the aliphatic side chain to the A-ring are almost identical. The affinities of the C-2 substituted analogues for VDR reflect the balance between the loss of water mediated H-bonds, additional van der Waals contacts, and the entropic effect. The methyl substituent is small enough not to affect the water molecules network while providing additional van der Waals contacts that explain the higher binding affinity of this analogue. The propyl and propoxy groups replace W1 and shift W2 into a more unfavorable position with a consequent loss or weakening of H-bonds, consistent with the lower binding affinity. The hydroxypropyl and hydroxypropoxy groups replace both W1 and W2, but their terminal hydroxyl groups maintain essential channel interactions. In summary, C-2 analogues take advantage of a water channel in VDR and provide a rationale approach for designing more potent ligands for increased stability.

While the crystal structures explain the affinity of these ligands, they do not explain the HL60 cell differentiation data. Indeed, **B** and **E** compounds lead to an increase of both stability and monocyte-like cells. In contrast, such a correlation is not observed for **D**. Our results highlight that the correlation between binding affinity and HL60 cell differentiation may not be predicted. Additional or unknown factors as well as tissue specificity are likely to be involved.

These new crystal structures with selected 2α-substituted 1α,-25-dihydroxyvitamin D₃ analogues provide correlations of 2α modifications of the A-ring with VDR affinity and the structural basis for the functional importance of the water channel molecules. The presence of similar water channels is observed in several other NRs (RAR, ER). Furthermore, the surface formed by the water channel of ERα has been shown to be part of a new peptide binding site that may function as a new coregulator recruitment site.[31] These selected 2α-substituted 1α,-25-dihydroxyvitamin D₃ analogues could recruit distinct coactivators to VDR in a temporal-regulated manner to modulate HL60 cell differentiation. Future experiments aimed at the identification of specific coregulators and determination of their kinetics of recruitment to VDR in response to these C-2α analogue-treated HL60 cells may lead to the discovery of new therapeutic targets.

Experimental Section

Purification and Crystallization. Purification and crystallization of the human VDR LBD complexes with five ligands were performed as previously described.[9] The LBD of the human VDR (residues 118−427 Δ166−216) was cloned in pET28b expression vector to obtain an N-terminal hexahistidine-tagged fusion protein and was overproduced in *E. coli* BL21 (DE3) strain. Cells were grown in LB medium and subsequently incubated for 6 h at 20°C with 1mM isopropyl thio-β-D-galactoside. The protein purification included a metal affinity chromatography step on a cobalt-chelating resin. The tag was removed by thrombin digestion overnight at 4°C, and the protein was further purified by gel filtration on a Superdex S200 16/60. The protein buffer prior to concentration of the protein contains 10 mM Tris, pH 7.5, 100 mM NaCl, and 5 mM dithiothreitol. The protein was concentrated to 10 mg/mL and incubated in the presence of a 5-fold excess of ligands. The purity and homogeneity of the protein were assessed by SDS−PAGE and native-PAGE. Crystals of complexes were obtained at 4 °C by vapor diffusion in hanging drops using crystals of VDR LBD−1α,25-(OH)₂D₃ as microseeds. The reservoir solutions contained 0.1 M Mes and 1.4 M ammonium sulfate at pH 6.0.

X-ray Data Collection and Processing. The crystals were mounted in fiber loops and flash-cooled in liquid ethane at liquid nitrogen temperature after cryoprotection with a solution containing the reservoir solution, 30% glycerol, and 5% PEG400. Data collection from a single frozen crystal was performed at 100 K at beamlines ID14-2, ID14-4, and ID23 of ESRF (Grenoble, France). The crystals were isomorphous and belonged to the orthorhombic space group $P2_12_12_1$ with the unit cell parameters as specified in Supporting Information. Data were integrated and scaled by using the HKL2000 program package.[32]

Structure Determination. The crystal structure of the VDR LBD complexes with five ligands were solved by molecular replacement using the known human VDR LBD−1α,25(OH)₂D₃ structure as a starting model. The omit maps from the refined atomic model of VDR LBD were used to fit the ligands to their electron density, as shown in Figure 3a. Anisotropic scaling, a bulk solvent correction, and restrained isotropic atomic *B*-factor refinement were used. The programs MOLREP,[33] CNS-SOLVE,[34] and O[35] were used for molecular replacement, structure refinement, and manual model building. Alternate cycles of maximum likelihood refinement and model fitting were subsequently performed to generate the final model of the complex. All data were included in the refinement (no δ cutoffs). All refined models showed unambiguous chirality for the ligands and no Ramachandran plot outliers according to PROCHECK.

All final models lack the first two N-terminal residues and the last four C-terminal residues. In addition, the final models of VDR−**C** and VDR−**D** complexes lack the Pro-374 residue, and the VDR−**F** complex lacks the Pro-373 and Pro-374 residues. In all VDR−ligand complexes, the electron density for residues 370−379 in loop 9−10 was low. For structure comparison, Cα traces of the models were superimposed using the lsq commands of O and default parameters. The figures were generated with Setor and Pymol.[36] The volume of ligand was calculated with GRASP.[37]

Assays for Induction of HL-60 Cell Differentiation. Experiments were conducted on the human cell line HL-60, which can be induced to differentiate to monocyte-like cells in response to the treatment with 1α,25(OH)₂D₃. Activity of the analogues on differentiation of HL-60 cells was estimated by nitroblue tetrazolium (NBT) reduction assay[38] with some modifications. HL-60 cells were grown at 37 °C in RPMI 1640 medium (Asahi Technologlass Co., Chiba, Japan) supplemented with 10% fetal bovine serum (Sigma, St. Louis, MO) in an atmosphere of 95% air and 5% CO₂. Cell culture (5 × 10⁵ cells/mL) was achieved in RPMI containing various concentrations (0, 10⁻¹⁰−10⁻⁶ M) of the analogues for 5 days. After the treatment, cells were harvested and suspended in Tyrode's solution (140 mM NaCl, 2.7 mM KCl, 1.1 mM MgCl₂, 1 mM CaCl₂, 0.45 mM NaH₂PO₄, 5.6 mM D-glucose, pH 7.4) containing 25 mM HEPES and 0.01% NBT (Dojindo Laboratories, Kumamoto, Japan). After preincubation at 37 °C for 7 min, phorbol 12-myristate 13-acetate (0.81 µM, Sigma, St. Louis, MO) was added to the cell suspension, which was further incubated for 30 min at 37 °C. Reaction was stopped by EDTA (2 mM), and then the percentage of positive cells (blue-stained cells) was determined using a hemocytometer. This experiment was performed three times for each analogue. The EC₅₀ value was estimated from the obtained dose response curve. Relative differentiation activity was calculated according to the following formula:

$$\text{relative differentiation activity} = \frac{\text{EC}_{50} \text{ of } 1\alpha,25\text{-dihydroxyvitamin D}_3}{\text{EC}_{50} \text{ of the analogue}} \times 100.$$

Binding Assays to the Bovine Thymus VDR. Bovine thymus VDR was obtained from a commercial supplier, and the affinity was evaluated according to the literature.[39]

Supporting Information Available: Crystallographic data and refinement statistics. This material is available free of charge via the Internet at http://pubs.acs.org.

References

(1) Laudet, V.; Gronemeyer H. *The Nuclear Receptor Facts Book*; Academic Press: London, 2002.

(2) Smith, C. L.; O'Malley, B. W. Coregulator function: a key to understanding tissue specificity of selective receptor modulators. *Endocr. Rev.* **2004**, *25*, 45−71.

(3) Bouillon, R.; Okamura, W. H.; Norman A. W. Structure−function relationships in the vitamin D endocrine system. *Endocr. Rev.* **1995**, *16*, 200−257.

(4) Beckman, M. J.; Deluca, H. F. Modern view of vitamin D3 and its medicinal uses. *Prog. Med. Chem.* **1998**, *35*, 1−56.

(5) Norman, A. W.; Mizwicki, M. T.; Norman, D. P. Steroid−hormone rapid actions, membrane receptors and a conformational ensemble model. *Nat. Rev. Drug Discovery* **2004**, *3*, 27−41.

(6) Lieberherr, M. Effects of vitamin D3 metabolites on cytosolic free calcium in confluent mouse osteoblasts. *J. Biol. Chem.* **1987**, *262*, 13168−13173.

(7) Hendy, G. N.; Hruska, K. A.; Mathew, S.; Goltzman, D. New insights into mineral and skeletal regulation by active forms of vitamin D. *Kidney Int.* **2006**, *69*, 218−223.

(8) Bouillon, R.; Verlinden, L.; Eelen, G.; De Clercq, P.; Vandewalle, M.; Mathieu, C.; Verstuyf, A. Mechanisms for the selective action of vitamin D analogs D. *J. Steroid Biochem. Mol. Biol.* **2005**, *97*, 21−30.

(9) Rochel, N.; Wurtz, J. M.; Mitschler, A.; Klaholz, B.; Moras, D. The crystal structure of the nuclear receptor for vitamin D bound to its natural ligand. *Mol. Cell* **2000**, *5*, 173−179.

(10) Tocchini-Valentini, G.; Rochel, N.; Wurtz, J. M.; Mitschler, A.; Moras, D. Crystal structures of the vitamin D receptor complexed to superagonist 20-epi ligands. *Proc. Natl. Acad. Sci. U.S.A.* **2001**, *98*, 5491−5496.

(11) Tocchini-Valentini, G.; Rochel, N.; Wurtz., J. M.; Moras, D. Crystal structures of the vitamin D nuclear receptor liganded with the vitamin D side chain analogues calcipotriol and seocalcitol, receptor agonists of clinical importance. Insights into a structural basis for the switching of calcipotriol to a receptor antagonist by further side chain modification. *J. Med. Chem.* **2004**, *47*, 1956−1961.

(12) Konno, K.; Fujishima, T.; Maki, S.; Liu, Z.; Miura, D.; Chokki, M.; Ishizuka, S.; Yamaguchi, K.; Kan, Y.; Kurihara, M.; Miyata, N.; Smith, C.; DeLuca, H. F.; Takayama, H. Synthesis, biological evaluation, and conformational analysis of A-ring diastereomers of 2-methyl-1,25-dihydroxyvitamin D(3) and their 20-epimers: unique activity profiles depending on the stereochemistry of the A-ring and at C-20. *J. Med.* Chem. **2000**, *43*, 4247−4265.

(13) Suhara, Y.; Nihei, K.; Kurihara, M.; Kittaka, A.; Yamaguchi, K.; Fujishima, T.; Konno, K.; Miyata, N.; Takayama, H. Efficent and versatile Synthesis of novel 2α-substituted 1α, 25-dihydroxyvitamin D₃ Analogues and their docking to vitamin D receptors. *J. Org. Chem.* **2001**, *66*, 8760−8711.

(14) Honzawa, S.; Suhara, Y.; Nihei, K.; Saito, N.; Kishimoto, S.; Fujishima, T.; Kurihara, M.; Sugiura, T.; Waku, K.; Takayama, H.; Kittaka, A. Concise Synthesis and biological activities of 2α-alkyl- and 2α-(ω-hydroxylalkyl)-20-epi-1α,25-dihydroxyvitamin D₃. *Bioorg. Med. Chem. Lett.* **2003**, *13*, 3503−3506.

(15) Saito, N.; Suhara, Y.; Kurihara, M.; Fujishima, T.; Honzawa, S.; Takayanagi, H.; Kozono, T.; Matsumoto, M.; Ohmori, M.; Miyata, N.; Takayama, H.; Kittaka, A. Design and efficient synthesis of 2α-(ω-hydroxylalkoxy)-1α, 25-dihydroxyvitamin D₃ analogues, including 2-epi-ED-71 and their 20-epimers with HL-60 cell differentiation activity. *J. Org. Chem.* **2004**, *69*, 7463−7471.

(16) Shimizu, M.; Yamamoto, K.; Mihori, M.; Iwasaki, Y.; Morizono, D.; Yamada, S. Two-dimensional alanine scanning mutational analysis of the interaction between the vitamin D receptor and its ligands: studies of A-ring modifed 19-norvitamin D analogus. *J. Steroid Biochem. Mol. Biol.* **2004**, *89−90*, 75−81.

(17) Honzawa, S.; Hirasaka, K.; Yamamoto, Y.; Peleg, S.; Fujishima, T.; Kurihara, M.; Saito, N.; Kishimoto, S.; Sugiura, T.; Waku, K.; Takayama, H.; Kittaka, A. Design, synthesis and biological evaluation of novel 1 alpha,25-dihydroxyvitamin D-3 analogues possessing aromatic ring on 2 alpha-position. *Tetrahedron* **2005**, *61*, 11253−11263.

(18) Rochel, N.; Tocchini-Valentini, G.; Egea, P. F.; Juntunen, K.; Garnier, J. M.; Vihko, P.; Moras, D. Functional and structural characterization of the insertion region in the ligand binding domain of the vitamin D nuclear receptor. *Eur. J. Biochem.* **2001**, *268*, 971−979.

(19) Wurtz, J. M.; Bourguet, W.; Renaud, J. P.; Vivat, V.; Chambon, P.; Moras, D.; Gronemeyer, H. A canonical structure for the ligand-binding domain of nuclear receptors. *Nat. Struct. Biol.* **1996**, *3*, 87−94.

(20) Takayama, H.; Konno, K.; Fujishima, T.; Maki, S.; Liu, Z.; Miura, D.; Chokki, M.; Ishizuka, S.; Smith, C.; DeLuca, H. F.; Nakagawa, K.; Kurobe, M.; Okanao, T. Systematic studies on synthesis, structural elucidation, and biological evaluation of A-ring diasteromers of 2-methyl-1α,25-dihydroxyvitamin D₃ and 20-epi-2methyl-1α,25-dihydroxyvitamin D₃. *Steroids* **2001**, *66*, 277−285.

(21) Muralidharan, K. R.; de Lera, A. R.; Isaeff, S. D.; Norman, A. W.; Okamura, W. H. Studies on the A-ring diasteromers of 1α,25-dihydroxyvitamin D₃. *J. Org. Chem.* **1993**, *58*, 1895−1899.

(22) Vanhooke, J. L.; Benning, M. M.; Bauer, C. B.; Pike, J. W.; DeLuca, H. F. Molecular structure of the rat vitamin D receptor ligand binding domain complexed with 2-carbon-substituted vitamin D3 hormone analogues and a LXXLL-containing coactivator peptide. *Biochemistry* **2004**, *43*, 4101−4010.

(23) Ciesielski, F.; Rochel, N.; Mitschler, A.; Kouzmenko, A.; Moras, D. Structural investigation of the ligand binding domain of the zebrafish VDR in complexes with 1α,25(OH)₂D₃ and Gemini: purification, crystallization and preliminary X-ray diffraction analysis. *J. Steroid Biochem. Mol. Biol.* **2004**, *89−90*, 55−59.

(24) Mizwicki, M. T.; Bishop, J. E.; Norman, A. W. Applications of the vitamin D sterol−vitamin D receptor (VDR) conformational ensemble model. *Steroids* **2005**, *70*, 464−471.

(25) Fujishima, T.; Kittaka, A.; Kurihara, M.; Saito, N.; Honzawa, S.; Kishimoto, S.; Sugiura, T.; Waku, K.; Takayama, H. 2,2-Functionalized analogues of 1alpha,25-dihydroxyvitamin D3, the potent inducers of cell differentiation. *J. Steroid Biochem. Mol. Biol.* **2004**, *89−90*, 89−92.

(26) Verlinden, L.; Verstuyf, A.; Verboven, C.; Eelen, G.; De Ranter, C.; Gao, L. J.; Chen, Y. J.; Murad, I.; Choi, M.; Yamamoto, K.; Yamada, S.; VanHaver, D.; Vandewalle, M.; De Clercq, P.; Bouillon, R. Previtamin D3 with a trans-fused decalin CD-ring has pronounced genomic activity. *J. Biol. Chem.* **2003**, *278*, 35476−35482.

(27) Vaisanen, S.; Ryhanen, S.; Saarela, J. T.; Maenpaa, P. H. Structure−function studies of new C-20 epimers pairs of vitamin D3 analogs. *Eur. J. Biochem.* **1999**, *261*, 706−713.

(28) Eelen, G.; Verlinden, L.; Rochel, N.; Claessens, F.; De Clercq, P.; Vandewalle, M.; Tocchini-Valentini, G.; Bouillon, R.; Verstuyf, A. Superagonistic action of 14-epi-analogs of 1,25-dihydroxyvitamin D explained by vitamin D receptor−coactivator interaction. *Mol. Pharmacol. Biol.* **2005**, *67*, 1566−1573.

(29) Malloy, P. J.; Pike, J. W.; Feldman, D. The vitamin D receptor and the syndrome of hereditary 1,25-dihydroxyvitamin D-resistant rickets. *Endocr. Rev.* **1999**, *20*, 156−188.

(30) Kittaka, A.; Kurihara, M.; Peleg, S.; Suhara, Y.; Takayama, H. 2α-(3-Hydroxypropyl)- and 2α-(3-hydroxypropoxy)-1α,25-dihydroxyvitamin D3 accessible to vitamin D receptor mutant related to hereditary vitamin D-resistant rickets. *Chem. Pharm. Bull.* **2003**, *51*, 357−358.

(31) Kong, E. J.; Helfring, N.; Gustafsson, J. A.; Treuter, E.; Hubbard, R. E.; Pike, C. W. Delineation of a unique protein−protein interaction site on the surface of the estrogen receptor. *Proc. Natl. Acad. Sci. U.S.A.* **2005**, *102*, 3593−3598.

(32) Otwinowski, Z.; Minor, W. Processing X-ray data collected in oscillation mode. *Methods Enzymol.* **1997**, *276*, 307−326.

(33) Vagin, A.; Teplyakov, A. *MOLREP*: an automated program for molecular replacement. *J. Appl. Crystallogr.* **1997**, *30*, 1022−1025.

(34) Brunger, A. T.; Adams, P. D.; Clore, G. M.; DeLano, W. L.; Gros, P.; Grosse-Kunstleve, R. W.; Jiang, J. S.; Kuszewski, J.; Nilges, M.; Pannu, N. S.; et al. Crystallography & NMR system: A new software suite for macromolecular structure determination. *Acta Crystallogr. D* **1998**, *54*, 905−921.

(35) Jones, T. A.; Zou, J. Y.; Cowan, S. W.; Kjeldgaard, M. Improved methods for building protein models in electron density maps and the location of errors in these models. *Acta Crystallogr. A* **1991**, *47*, 110−119.

(36) DeLano, W. L. *The PyMOL Molecular Graphics System*; DeLano Scientific: San Carlos, CA, 2002.

(37) Nicholls, A.; Sharp, K. A.; Honig, B. Protein folding and association: insights from the interfacial and thermodynamic properties of hydrocarbons. *Proteins* **1991**, *11*, 281−296.

(38) Collins, S. J.; Ruscetti, F. W.; Gallagher, R. E.; Gallo, R. C. Normal functional characteristics of cultured human promyelocytic leukemia cells (HL-60) after induction of differentiation by dimethylsulfoxide. *J. Exp. Med.* **1979**, *149*, 969−974.

(39) Ono, K.; Yoshida, A.; Saito, N.; Fujishima, T.; Honzawa, S.; Suhara, Y.; Kishimoto, S.; Sugiura, T.; Waku, K.; Takayama, H.; Kittaka A. Efficient synthesis of 2-modified 1α,25-dihydroxy-19-norvitamin D_3 with Julia olefination: high potency in induction of differentiation on HL-60 cells. *J. Org. Chem.* **2003**, *68,* 7407−7415.